Genetics and Molecular Research

Proteomic changes in maize as a response to heavy metal (lead) stress revealed by iTRAQ quantitative proteomics

G.K. Li[1,3]*, J. Gao[4]*, H. Peng[1,2], Y.O. Shen[1], H.P. Ding[1], Z.M. Zhang[1], G.T. Pan[1] and H.J. Lin[1]

[1]Key Laboratory of Biology and Genetic Improvement of Maize in Southwest Region, Ministry of Agriculture,
Maize Research Institute of Sichuan Agricultural University, Wenjiang, Sichuan, China
[2]Sichuan Tourism University, Chengdu, Sichuan, China
[3]Guangdong Provincial Key Laboratory of Crops Genetics and Improvement, Guangdong Academy of Agricultural Sciences, Crop Research Institute, Guangzhou, China
[4]Key Laboratory of Tumor Immunopathology,
Institute of Pathology and Southwest Cancer Center, Southwest Hospital,
Third Military Medical University, Ministry of Education, Chongqing, China

*These authors contributed equally to this study.
Corresponding authors: G.T. Pan / H.J. Lin
E-mail: pangt1956@aliyun.com / linhj521@gmail.com

Genet. Mol. Res. 15 (1): gmr.15017254
Received September 14, 2015
Accepted November 5, 2015
Published January 26, 2016
DOI http://dx.doi.org/10.4238/gmr.15017254

ABSTRACT. Lead (Pb), a heavy metal, has become a crucial pollutant in soil and water, causing not only permanent and irreversible health problems, but also substantial reduction in crop yields. In this study, we conducted proteome analysis of the roots of the non-hyperaccumulator inbred maize line 9782 at four developmental stages (0, 12, 24, and 48 h) under Pb pollution using isobaric tags for relative and absolute quantification technology. A total of 252, 72 and 116 proteins were differentially expressed between M12 (after 12-h Pb treatment) and CK (water-mocked

treatment), M24 (after 24-h Pb treatment) and CK, and M48 (after 48-h Pb treatment) and CK, respectively. In addition, 14 differentially expressed proteins were common within each comparison group. Moreover, Cluster of Orthologous Groups enrichment analysis revealed predominance of the proteins involved in posttranslational modification, protein turnover, and chaperones. Additionally, the changes in protein profiles showed a lower concordance with corresponding alterations in transcript levels, indicating important roles for transcriptional and posttranscriptional regulation in the response of maize roots to Pb pollution. Furthermore, enriched functional categories between the successive comparisons showed that the proteins in functional categories of stress, redox, signaling, and transport were highly up-regulated, while those in the functional categories of nucleotide metabolism, amino acid metabolism, RNA, and protein metabolism were down-regulated. This information will help in furthering our understanding of the detailed mechanisms of plant responses to heavy metal stress by combining protein and mRNA profiles.

Key words: Pb pollution; Isobaric tags for relative and absolute quantification; Differentially expressed proteins

INTRODUCTION

Plants are frequently subjected to various environmental stresses, such as cold, heat, drought, flooding, salt, light, and pollutants (including heavy metals) (Tester and Bacic, 2005), which have marked effects on plant vigor and crop yields. Recent studies have shown that environmental pollution due to heavy metals represents a serious threat to living organisms. Lead (Pb) has become the most important metal pollutant of the environment because of widespread heavy metal pollution from agriculture, industry, and other human activities (Valko et al., 2005). Plants have developed various abilities to cope with and adapt to stress conditions by changing levels of protein, displaying a relative abundance of stress-responsive proteins in the proteome. To investigate the expression and modification of all proteins in an organism, high-throughput analyses for proteome studies have been developed, aided by advancements in mass spectrometry, genome sequencing, and bioinformatics (Miernyk and Hajduch, 2011).

Maize has a relatively high proportion of its biomass in its roots; therefore, maize could be an important model to study the phytoremediation of Pb-contaminated soil. Previous studies have indicated that a range of gene regulatory mechanisms control the accumulation capacity of Pb in plants, including transcription factors, transport proteins, and some critical genes, which were activated in response to both biotic and abiotic stresses and were involved in certain signal transduction and secondary metabolite pathways (Atkinson and Urwin, 2012; Thapa et al., 2012; Fan et al., 2013). In a previous study, we assayed Pb contents in the roots and aboveground parts of 19 inbred lines of maize seedlings. We selected the non-hyperaccumulator maize germplasm 9782 with Pb accumulation in roots, stems, and leaves under Pb conditions, and compared these individuals with the hyperaccumulator 178 (Zhang et al., 2012). In addition, transcriptomic changes during maize root development in response to Pb were investigated in the non-hyperaccumulator maize germplasm 9782 using RNA sequencing (Gao et al., 2015), as well as the dynamics of

DNA methylation in maize germplasm 9782 roots under Pb stress (Ding et al., 2014). However, proteomic alteration profiling involved in various metabolic functions associated with Pb pollution is still uncertain.

In our research, considering that limited information is available with regard to the response of maize roots to Pb pollution, we generated a transcriptome, measuring the relative or absolute expression of protein during the response of maize roots to Pb stress. The recently developed isobaric tag for relative and absolute quantification (iTRAQ) system was used to accurately quantify differentially expressed proteins (DEPs), by measuring peak intensities of reporter ions in tandem mass spectrometry (MS/MS) spectra. DEPs were identified using iTRAQ and the expression patterns at the protein level correlated with transcript levels were investigated.

MATERIAL AND METHODS

Plant materials and experimental design

Seeds of maize (*Zea mays*) inbred line 9782 were sown on filter paper saturated with distilled water and incubated at 26°C in the dark. Seedlings with uniform growth were selected after three days, transplanted into an aerated complete nutrient solution (see **Table S1**), and grown in a growth chamber as follows: seedlings were maintained for three days with a 14-h light/10-h dark photoperiod at 26°C and a relative humidity of 70%. After that, the maize seedlings were randomly divided into four groups. CK (water-mocked treatment)-grown (C1A) seedlings were grown only in half-strength Hoagland solution, while Pb1000-grown seedlings were grown in CK + Pb1000 [1000 mg/L $Pb(NO_3)_2$] to achieve Pb stress for 12, 24, and 48 h, respectively.

Protein extraction

Protein was extracted using the trichloroacetic acid (TCA)/acetone method (Sheoran et al., 2009) with modifications. Tuber cubes with 10% polyvinyl-polypyrrolidone were ground in liquid nitrogen and suspended in 5 volumes of chilled (20°C) acetone containing 10% TCA (w/v). The homogenate was then precipitated for 2 h at 20°C and centrifuged at 20,000 *g* for 20 min at 4°C. The supernatant was carefully removed, and the protein pellets were washed three times with chilled acetone. Washed protein pellets were air-dried and dissolved in 500 mL 0.5 M triethylammonium bicarbonate (TEAB) for 15 min under 200 W sonication, and centrifuged at 30,000 *g* for 20 min at 4°C. Then, the disulfide bonds were reduced in 10 mM dithiothreitol at 56°C for 1 h and followed by alkylation in 55 mM iodoacetamide for 45 min. The supernatant was precipitated overnight at 20°C by the addition of 5 volumes of chilled acetone before centrifuging. The air-dried pellet was dissolved in 500 mL 0.5 M TEAB for 15 min under 200 W sonication. The supernatant was collected as the soluble protein fraction after centrifugation at 30,000 *g* for 15 min at 4°C. Protein concentration was estimated as a standard using the Bio-Rad protein assay kit (Bio-Rad, Hercules, CA, USA) with bovine serum albumin. The quality of each protein sample was evaluated using sodium dodecyl sulfate-polyacrylamide gel electrophoresis.

iTRAQ labeling and mass spectrometry analysis

iTRAQ labeling and mass spectrometry analysis were performed at the Beijing Genomics Institute (Shenzhen, China) according to the method described by Gan et al. (2007). From each

sample, 100 µg reduced and alkylated protein was digested using sequencing-grade trypsin (Promega Corporation, Beijing) and labeled using iTRAQ 8-plex kits (Applied Biosystems, USA) according to the manufacturer protocol. M12 samples were labeled with reagent 113 and 118, M24 samples were labeled with reagent 114 and 119, and M48 samples were labeled with reagent 115 and 121. After labeling and quenching, the samples were combined and further fractionated by strong cation exchange (SCX) chromatography on an Ultramax SCX column using Shimadzu LC-20AB HPLC. The fractionated samples were analyzed by nano-LC-MS/MS. Peak lists were generated with the Proteome Discoverer 1.3 software.

Proteomic data analysis

Proteins were identified and quantified simultaneously using the Mascot software (version 2.3.02, Matrix Science), and then searched against the maize protein database with the following search parameters: trypsin was chosen as the enzyme with one missed cleavage allowed; fixed modifications of carbamidomethylation at Cys; variable modifications of oxidation at Met; peptide tolerance was set at 0.05 Da and MS/MS tolerance at 0.1 Da; and monoisotopic mass was chosen. iTRAQ 8-plex was chosen for quantification during the search. Protein quantitation was performed at the peptide level by following the procedures described in http://www.matrixscience.com/help/quant_statistics_help.html. Proteins with changes of 1.5-fold or greater between successive comparisons and a P value of statistical evaluation less than 0.05 were determined as differentially expressed proteins. The MapMan 3.6.0RC1 tool (http://mapman.gabipd.org/web/guest) was used to display expression profiles at the pathway level. Expression values were calculated based on a log2 scale and used to visualize the metabolic processes.

Comparison of protein and mRNA expression profiles

To compare changes in protein abundance with alterations in transcript levels, we conducted RNA sequencing experiments using the same materials as described in protein extraction. RNA extraction (Cat. No. 15596-026, Invitrogen) and RNA sequencing library construction (Illumina protocol) were performed following manufacturer instructions. In this study, the quantified proteins were quantitatively compared and clustered into four groups based on mRNA and protein levels. These groups were i) mRNA and protein levels having the same trends, ii) mRNA and protein levels having opposite change trends, iii) protein levels changing significantly while the mRNA was unchanged, and iv) mRNA levels changing significantly while the protein remains unchanged. Pearson correlation tests were conducted using expression ratios of M12 *vs* CK, M24 *vs* CK, and M48 *vs* CK, respectively.

RESULTS

Overview of quantitative proteome analysis

The proteome of maize roots responsive to Pb pollution were quantitatively cataloged using iTRAQ technology. Briefly, proteins were extracted, digested, and iTRAQ-labeled in solution. Of those, unlabeled peptides were excluded from the data sets; iTRAQ-labeled peptides were analyzed using liquid chromatography combined with tandem mass spectroscopy. Of the 352,944

mass spectra obtained that matched to special peptides, low-scoring spectra were eliminated by data filtering, and 24,151 high-scoring unique spectra were identified. Of those, 6029 unique peptides were identified from 7442 peptides, corresponding to 2440 proteins in the four samples (Figure 1A). In terms of protein mass distribution, good coverage (averages of 10-16% of the total proteins in each protein mass group) was obtained for a wide protein mass (PS range for proteins larger than 10 kDa and less than 70 kDa) (Figure 1B). In addition, peptide coverage in the proteins was identified; more than 48% of the proteins had more than 5% of sequence coverage (Figure 1C). Moreover, most of the proteins were identified with good distribution of sequence coverage; 70% of the proteins had over 10% of the sequence coverage and 56% were with 20% of the sequence coverage (Figure 1D). To quantify their abundance, a subset protein was identified by at least two peptides (**Table S1**). Of the proteins detected, 2112, 2091, 2236, 2238, 2217, and 2076 were identified from samples of M12_re1, M12_re1, M24_re1, M24_re2, M48_re1, and M48_re2, respectively. Comparisons between various biological replicates are shown in Figure 2 to demonstrate analytical reproducibility. We labeled and mixed each pair of Pb-treated sample and its control for proteomic analysis; the results showed that 96.09, 98.55, and 96.34% of the proteins were detected in all six biological samples for M12, M24, and M48, respectively (Figure 2). In addition, two biological replicates of Pb1000-treated samples were labeled and mixed for proteomic analysis, and the percentage of proteins revealed, suggesting that biological noise was reasonably low and the analysis is reliable for protein identification (Figure 3).

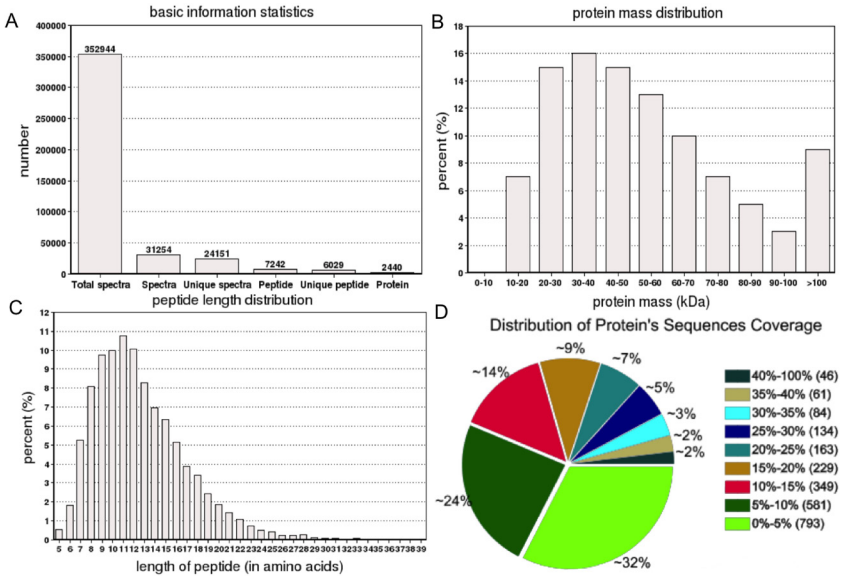

Figure 1. Analysis of maize roots responsive to Pb pollution proteome profile by iTRAQ. Total spectra are the secondary mass spectrums, and spectra are the secondary mass spectrums after quality control. Unique Peptide is the identified peptides that belong only to a group of proteins, and protein is identified by the Mascot 2.3.02 software. **A.** High scoring unique spectra matched to special peptides were obtained, unique peptides were identified from peptides corresponding to proteins in the four samples were identified. **B.** Obtaining of good coverage of protein mass distribution. **C.** Identification of length peptide coverage in the proteins. **D.** Identification of proteins with good distribution of peptide coverage. Total Spectra is the total for the secondary spectra, Spectra is the number of matched spectra, Unique Spectra is the the number of spectrum to matched unique peptides, Peptide is the number of peptides by identify, Unique Peptide is the sequence number of the specific peptide by identify is segments, Protein is the the amount of protein by identify.

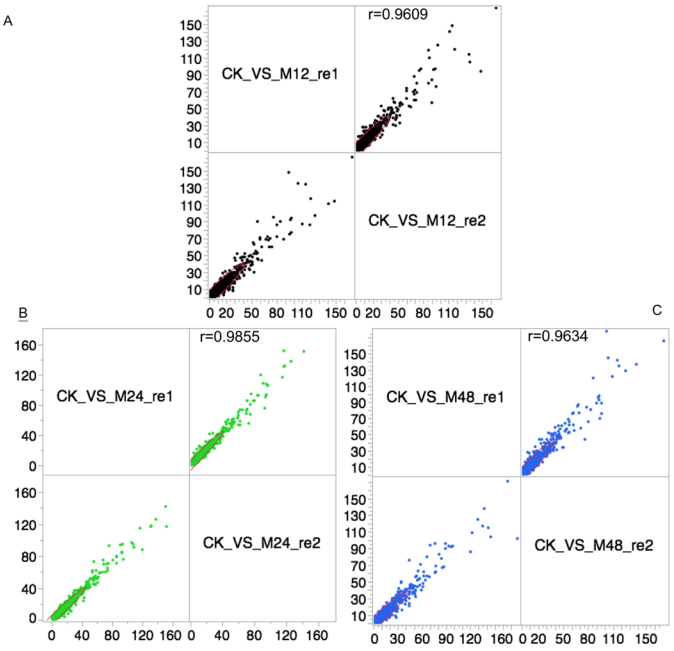

Figure 2. Comparisons between various biological replicates to demonstrate the analytical reproducibility, each pair of Pb-treated samples and its control for proteomic analysis were labeled in all six biological samples for M12, M24 and M48, respectively.

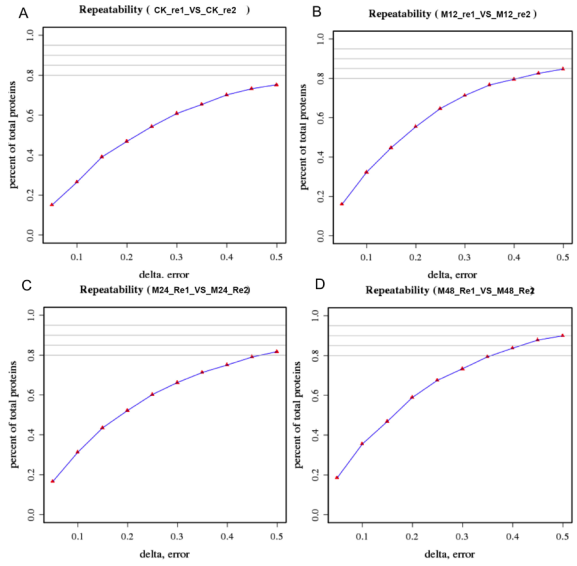

Figure 3. Different proteins identified by two biological replicates. To further elucidate the global function of proteins responsive to Pb pollution, the detected proteins were categorized into different functional groups based on the Cluster of Orthologous Groups (COG) database. Expect for general function prediction only, the percentages of proteins involved in posttranslational modification, protein turnover, and chaperones were dominant, indicating that post-transcriptional regulation plays an vital roles in maize roots responsive to Pb pollution (Figure 4).

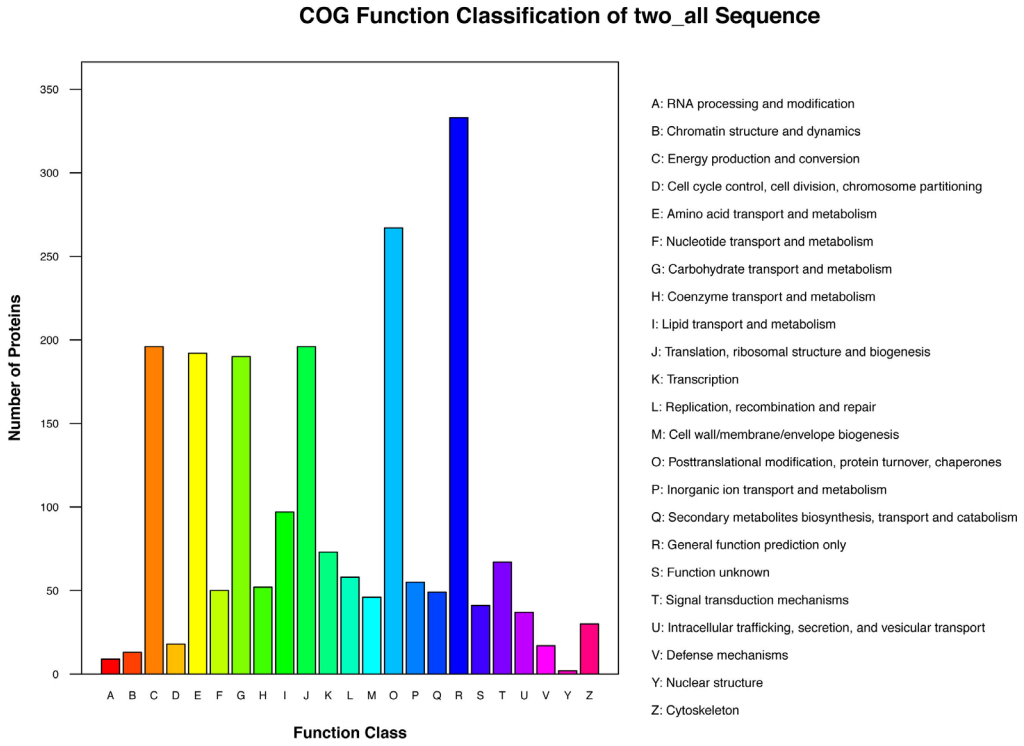

Figure 4. Cluster of Orthologus Groups (COG) analysis of differentially expressed proteins in maize roots responsive to Pb pollution. Shown above is the classification of these proteins in different categories based on biological process.

Functional annotation analysis of differences in proteome

To further identify the DEPs in maize roots under Pb stress, proteins with > 1.5-fold difference and P value < 0.05 were regarded as being differentially expressed (Gan et al., 2007). DEP levels of the developmental stages after Pb pollution were compared with those of the mock-treatment control (M12 *vs* CK, M24 *vs* CK and M48 *vs* CK). Of these, 252 proteins were screened as differentially expressed between M12 and CK, including 115 proteins that were up-regulated and 137 that were down-regulated; 72 proteins experienced significant up- (35) or down-regulation (37) between M24 and CK and 116 proteins experienced significant up- (57) or down-regulation (59) between M48 and CK (Table 1). In addition, 14 DEPs were found to be common between M12 and CK, M24 and CK, and M48 and CK. Cluster analysis showed that 4 DEPs were increased and 10 DEPs were induced after Pb1000 treatment. However, most of them were significantly increasing during the maize roots' response to Pb treatment (Figure 5). Interestingly, based on the differentially expressed genes identified by RNAseq in our study, most DEPs also were identified in the M12 *vs* CK comparison, suggesting that M12 represents the most active period of the response of maize roots to Pb stress.

Table 1. DEPs between M48 and CK.

Accession No.	Cov	Unique Spectrum	Unique Peptide	Log2 (Treat/CK)	Description
GRMZM2G024354_P01	19.6	17	1	2.43	60S ribosomal protein L15
GRMZM2G358059_P01	24.9	3	1	2.41	Calreticulin2
GRMZM2G015361_P01	27.6	23	5	2.11	GTP binding
GRMZM2G039639_P01	4.8	7	1	1.79	Protein P21
GRMZM2G002825_P01	15.8	17	2	1.59	Actin-depolymerizing factor 3
GRMZM2G014240_P01	12.3	7	2	1.38	Inorganic diphosphatase activity
AC233895.1_FGP001	17.8	28	7	1.08	Proliferation-associated protein 2G4
GRMZM2G052562_P01	2.5	6	1	0.93	Zea nodulation homolog1
GRMZM2G036099_P03	13.6	8	2	0.91	Calcium ion binding
GRMZM2G162426_P01	3.4	6	3	0.89	Catalytic activity
GRMZM5G877500_P01	5.1	5	2	0.87	Catalytic activity
GRMZM2G033208_P01	14.4	38	7	0.80	Catalytic activity
GRMZM2G015361_P01	27.6	23	5	0.70	GTP binding
GRMZM2G113696_P01	18.8	21	3	0.69	Translation initiation factor 5A
GRMZM2G085967_P01	29.0	65	8	0.69	Peroxidase 39
GRMZM2G358059_P01	24.9	3	1	0.66	Calreticulin2
GRMZM2G008247_P01	20.2	12	1	0.65	Beta-D-glucosidase precursor
GRMZM2G058675_P02	29.3	42	9	0.65	Restorer of fertility2
GRMZM2G109677_P03	15.2	37	7	0.62	Structural constituent of ribosome
GRMZM2G109677_P03	15.2	37	7	0.62	Structural constituent of ribosome
GRMZM2G178693_P01	14.4	15	3	0.60	Plasma membrane intrinsic protein
GRMZM2G154169_P01	14.5	9	2	-0.62	GRF-interacting factor 2-like
GRMZM2G107073_P01	11.7	23	4	-0.63	Glycoside hydrolase, family 28
GRMZM2G000326_P01	38.6	18	2	-0.63	Subtilisin-chymotrypsin inhibitor CI-1B
GRMZM2G305046_P01	28.9	12	1	-0.64	Histone2A1
GRMZM2G038636_P01	6.4	12	2	-0.68	Cysteine protease
GRMZM2G050514_P01	33.1	10	4	-0.68	Glutamine synthetase
AC197758.3_FGP004	15.9	21	3	-0.70	Peroxidase 52
GRMZM2G145440_P01	7.5	3	1	-0.73	Receptor kinase 1
GRMZM2G117989_P01	5.1	9	1	-0.81	Defense response to bacterium
GRMZM2G146246_P02	36.2	21	6	-0.82	Glutathione S-transferase4
GRMZM2G003306_P01	29.5	10	1	-0.83	Nucleosome
GRMZM2G057608_P01	28.7	16	3	-0.90	40S ribosomal protein S25-1
GRMZM2G156632_P01	9.8	12	1	-1.02	WIP1
GRMZM2G039639_P01	4.8	7	1	-1.03	Protein P21
GRMZM2G374971_P01	16.7	14	3	-1.13	Stress-induced protein1
GRMZM2G005633_P02	21	8	3	-1.15	Chitinase activity
GRMZM2G304442_P01	20.1	15	3	-1.35	Extracellular region
GRMZM2G075624_P01	24.0	16	2	-1.35	Translationally controlled tumor protein-like Protein
GRMZM2G078314_P01	16.9	4	1	-1.36	Nucleosome
GRMZM2G031545_P01	23.6	15	4	-1.44	Elongation factor 1-delta 1
GRMZM2G057608_P01	28.7	16	3	-1.49	40S ribosomal protein S25-1
GRMZM2G051879_P03	28.3	2	2	-1.91	Nucleosome
GRMZM2G158568_P01	11.4	7	2	-1.97	60S ribosomal protein L31
GRMZM2G117989_P01	5.1	9	1	-2.77	Defense response to bacterium
GRMZM2G083016_P01	15.7	6	2	-13.35	Phosphoglycerate kinase activity

Accession represent the protein code; coverage values represent the coverage (%) of each protein assigned by a peptides; unique peptide represent the unique peptide align to the protein; CK *vs* M48 represent the protein abundance at CK is compared to that at M48.

To further study the function of proteins related to Pb stress responsiveness, DEPs were also clustered according to expression changes during the developmental stages after Pb pollution-most proteins between M12 *vs* CK, M24 *vs* CK, and M48 *vs* CK demonstrated forward expression patterns using the MapMan program. Additionally, enriched functional categories between the successive comparisons showed that the proteins in functional categories of stress, redox, signaling, and transport were highly up-regulated, while proteins in functional categories of nucleotide metabolism, amino acid metabolism, RNA, and protein metabolism were down-regulated (Figure 6).

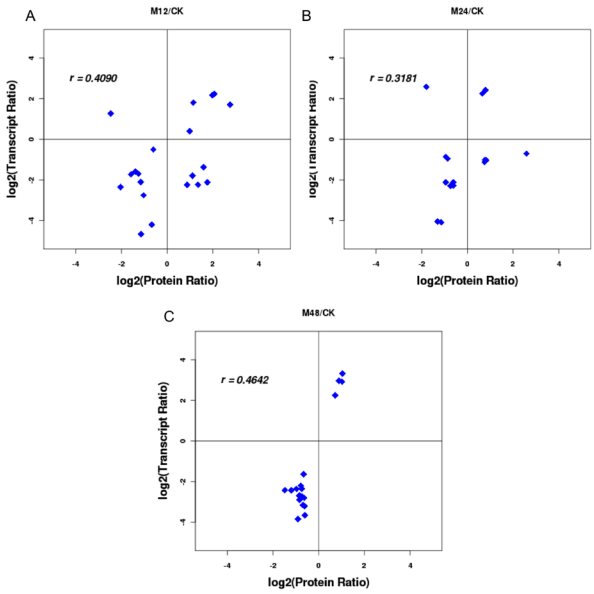

Figure 5. Common DEPs identified shared between each group, such as M12 *vs* CK, M24 *vs* CK and M48 *vs* CK. Cluster analysis showed increased and decreased DEPs induced by Pb treatment.

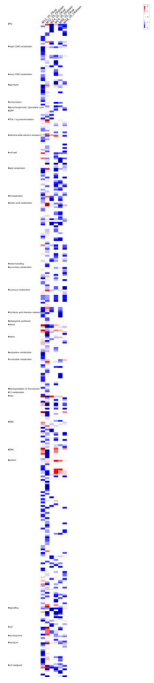

Figure 6. Differentially expressed proteins (DEPs) corresponded to expression changes during the developmental stages after Pb pollution. Clustered and enriched functional categories between the successive comparisons were conducted using MapMan program.

These results suggested that the stress and redox-related metabolism was mainly activated during the developmental stages after Pb pollution, and the metabolites, along with related signaling pathway and transport proteins, also increased to respond to Pb1000 treatment (**Table S2**).

Comparison of transcriptome and proteome expression

RNA sequencing provided the following numbers of high-quality clean reads from the respective stages: 19,562,150 from CK, 19,171,257 from M12, 19,248,546 from M24, and 17,813,916 from M48. These corresponded to 17,707, 17,440, 16,998, and 16,586 genes identified in maize roots at the four developmental stages (0, 12, 24, and 48 h), respectively. Also, 2825, 2626, 2161, and 2260 stage-specific genes at successive time points were screened, based on the absolute fold change value of log2 ratio >1 with $P < 0.001$ and FDR < 0.001 (data not shown).

To compare changes in protein abundance with alterations in transcript levels in maize roots responsive to Pb1000 treatment, the correlation between protein and mRNA expression profiles were further comprehensively investigated by comparing M12 *vs* CK, M24 *vs* CK, and M48 *vs* CK. Of 252 proteins that changed significantly in terms of abundance between M12 *vs* CK, only 41 of their corresponding transcripts were found to be differentially expressed. For M24 *vs* CK and M48 *vs* CK, of 72 and 116 proteins corresponding to 19 and 37 transcripts, respectively, some DEPs have the same or opposite change trends with their association mRNA in transcriptome level, some DEPs were significantly changed in proteasome level but the cognate mRNAs were not significantly changed. (Table 2). Next, the correlation between differentially expressed proteins and mRNAs was comprehensively investigated in the comparison of M12 *vs* CK, M24 *vs* CK, and M48 *vs* CK. Concordance tests revealed a positive correlation of r of 0.409, 0.318, and 0.4642 between protein and mRNAs for the significant change (Figure 7). This indicated that a change in transcript abundance may or may not translate into changes in protein level. Posttranscriptional regulatory processes such as protein-protein interactions, redox systems, processes of reversible phosphorylation, and some mediatory molecules may affect the efficiency of translation.

DISCUSSION

DEPs between Pb1000-grown and control groups

In the current study, the effects of heavy metal lead (Pb) on the proteome was investigated using quantitative proteomics to uncover Pb-regulated protein regulatory mechanisms in maize roots. However, previous studies have shown that transcription and translation do not always correlate well with each other. Therefore, our proteomic analysis may reveal novel players involved in heavy metal regulatory pathways. The iTRAQ method was used to identify putative DEPs potentially responsive to heavy metal pollution, and 14 DEPs were identified as being common within each comparison group (M12 *vs* CK, M24 *vs* CK, M48 *vs* CK). Of these 14 common DEPs in all examined time points, two plasma membrane intrinsic proteins (GRMZM2G178693_P01 and GRMZM2G154628_P01) were identified among the proteins that were up-regulated in M24 Pb-pollution conditions and then down-regulated in M48. Plasma membrane intrinsic proteins (PIPs), a subfamily of aquaporins, can control the translocation of water across the membrane. Previous studies have reported that, in various plant species, gene expression and function of

Table 2. Expression trend analysis of differential expression protein and mRNAs.

Protein	Peptide No.	Score	Quantition	Gene ID	log2 (treat/CK)	Trend	Description
GRMZM2G008748_P02	3	1074	0.465	GRMZM2G008748	-1.09	Same	LOC100191612
GRMZM2G015401_P01	39	810	0.3	GRMZM2G015401	-1.45	Same	Transporter activity
GRMZM2G024354_P01	17	677	0.185	GRMZM2G024354	-1.05	Same	60S ribosomal protein L15
GRMZM2G032564_P01	3	220	0.639	GRMZM2G032564	-1.64	Same	60S ribosomal protein L34
GRMZM2G074743_P01	4	66	2.081	GRMZM2G074743	3.33	Same	alternative oxidase AOX3 precursor
GRMZM2G156632_P01	12	284	2.033	GRMZM2G156632	1.40	Same	Bowman-Birk type wound-induced proteinase inhibitor WIP1
GRMZM2G145440_P01	3	145	1.659	GRMZM2G145440	2.25	Same	BRASSINOSTEROID INSENSITIVE 1-associated receptor kinase 1
GRMZM2G168552_P01	8	165	3119.326	GRMZM2G168552	2.73	Same	Bundle sheath cell specific protein 1
GRMZM2G043336_P01	7	139	0.585	GRMZM2G043336	-1.87	Same	Carbon fixation
GRMZM2G005633_P02	8	396	2.226	GRMZM2G005633	1.80	Same	Chitinase activity
GRMZM2G117989_P01	9	108	1.751	GRMZM2G117989	2.42	Same	Defense response to bacterium
GRMZM2G060952_P01	21	492	0.56	GRMZM2G060952	-2.90	Same	Deoxymugineic acid synthase1
GRMZM2G050514_P01	10	635	1.597	GRMZM2G050514	2.25	Same	Glutamine synthetase
GRMZM2G107073_P01	23	646	1.543	GRMZM2G107073	1.18	Same	Glycoside hydrolase, family 28
GRMZM2G015361_P01	23	574	0.617	GRMZM2G015361	-1.69	Same	GTP binding
GRMZM2G120962_P01	11	1147	0.609	GRMZM2G120962	-2.75	Same	Hydrolase activity, hydrolyzing O-glycosyl compounds
GRMZM2G162486_P01	7	574	1.862	GRMZM2G162486	2.96	Same	IN2-1 protein
GRMZM2G014240_P01	7	688	0.588	GRMZM2G014240	-2.20	Same	Inorganic diphosphatase activity
GRMZM2G156861_P01	9	3051	0.653	GRMZM2G156861	-2.12	Same	Lipoxygenase
GRMZM2G156861_P02	55	2424	0.52	GRMZM2G156861	-2.12	Same	Lipoxygenase
GRMZM2G085967_P01	65	2741	0.621	GRMZM2G085967	-3.16	Same	Peroxidase 39
GRMZM2G178693_P01	15	396	0.661	GRMZM2G178693	-1.45	Same	Plasma membrane intrinsic protein
GRMZM2G154628_P01	9	1085	0.606	GRMZM2G154628	-1.39	Same	Plasma membrane intrinsic protein2
GRMZM2G025105_P01	9	112	3.12	GRMZM2G025105	1.47	Same	Polygalacturonase inhibitor
GRMZM2G035599_P01	3	111	0.406	GRMZM2G035599	-4.04	Same	Ribose-5-phosphate isomerase
GRMZM2G374971_P01	14	266	2.187	GRMZM2G374971	1.51	Same	Stress-induced protein1
GRMZM2G003384_P01	4	996	0.46	GRMZM2G003384	-1.03	Same	Structural constituent of ribosome
GRMZM2G430902_P01	13	828	0.612	GRMZM2G430902	-1.27	Same	Voltage-gated chloride channel activity
GRMZM2G052562_P01	6	122	0.361	GRMZM2G052562	-2.42	Same	Zea nodulation homolog1
GRMZM2G151252_P01	10	1943	1.868	GRMZM2G151252	-1.08	Opposite	40S ribosomal protein S24
GRMZM2G043300_P01	4	120	2.052	GRMZM2G043300	-1.56	Opposite	Chemocyanin
AC234156.1_FGP005	11	231	2.172	AC234156.1_FG005	-1.80	Opposite	Fasciclin-like arabinogalactan protein 7
GRMZM2G078314_P01	4	87	2.563	GRMZM2G078314	-2.23	Opposite	Nucleosome
GRMZM2G027217_P01	5	180	3.412	GRMZM2G027217	-2.13	Opposite	Peroxidase activity
GRMZM2G410175_P01	13	1246	2.237	GRMZM2G410175	-6.35	Opposite	Peroxidase activity
GRMZM2G341410_P01	6	175	2.097	GRMZM2G341410	-1.04	Opposite	Protein binding
GRMZM2G353103_P01	10	394	3.644	GRMZM2G353103	-1.06	Opposite	Structural constituent of ribosome
GRMZM5G852185_P04	4	254	3.012	GRMZM5G852185	-1.07	Opposite	Structural constituent of ribosome
GRMZM2G064753_P01	7	198	1.565	GRMZM2G064753	-1.07	Opposite	Structural constituent of ribosome
GRMZM2G373522_P01	12	149	1.665	GRMZM2G373522	-1.03	Opposite	Dehydrin
GRMZM2G342515_P01	5	1826	1.724	GRMZM2G342515	-1.02	Opposite	Histone 2B5
GRMZM2G305046_P01	12	720	1.562	GRMZM2G305046	-1.80	Opposite	Histone2A1
GRMZM2G003306_P01	10	807	1.777	GRMZM2G003306	-1.03	Opposite	Nucleosome
GRMZM2G039639_P01	7	179	0.289	GRMZM2G039639	2.58	Opposite	Protein P21
GRMZM2G469304_P01	9	23	1.697	GRMZM2G469304	-1.12	Opposite	Ternary complex factor MIP1

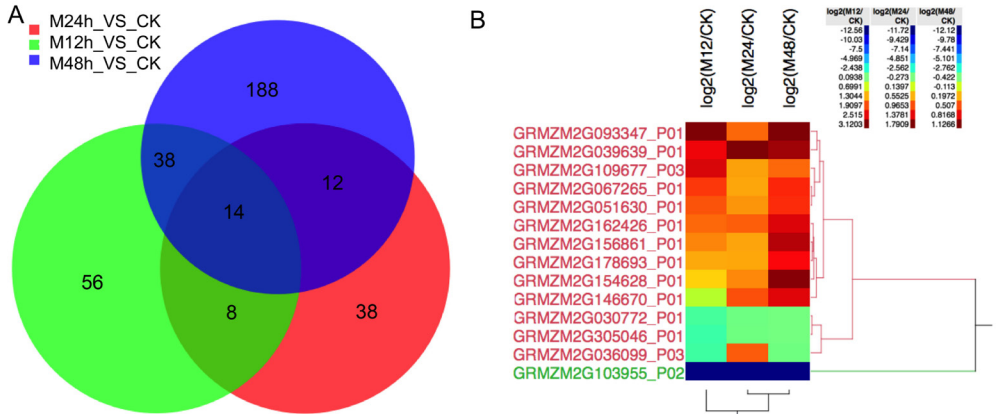

Figure 7. Correlation analysis between differentially expressed proteins and mRNA was comprehensively investigated in the comparison of each group, such as M12 *vs* CK, M24 *vs* CK and M48 *vs* CK. Concordance tests between protein and mRNAs for the significantly change were also conducted.

PIPs can be modulated by heavy metals such as cadmium, copper, and mercury (Guo et al., 2006). Expression of PsPIP2-1 showed an increasing trend after $HgCl_2$ [mercury (II) chloride] treatment in *Pisum sativum* (Beaudette et al., 2007), whereas copper stress genes encoding plasmalemma PIP were down-regulated under copper application in *Populus deltoides* roots (Guerra et al., 2009). Similarly, 15 tags annotated to PIPs were significantly down-regulated, while two tags annotated to *Arabidopsis* PIPs were up-regulated in response to cadmium stress in *Solanum torvum*. Moreover, coexpression of nonfunctional ZmPIP1;1 and ZmPIP1;2 isoforms with functional ZmPIP2 protein could enhance their aquaporin activity significantly in maize (Fetter et al., 2004). Further study suggested that PIP1 trafficking would be required for the plasma membrane by PIP1-PIP2 interaction, thereby modulating plasma membrane permeability (Zelazny et al., 2007). We demonstrated that PIPs might facilitate the transport of molecules by modulating plasma membrane permeability in response to Pb pollution.

In addition, most of these down-regulated proteins are metal-ion binding, involved in heavy metal detoxification systems by the activation of metal ion transport pathways; for example, manganese ion binding (GRMZM2G030772_P01) and calcium ion binding (GRMZM2G036099_P03). Transporter proteins mediate metal uptake in root cells and metal transfer between cells and organs. Metal transporters are also involved in metal detoxification by mediating the transport of metals from the cytosol to the vacuolar compartment (Salt and Wagner, 1993; Salt and Rauser, 1995; Rea, 1999).

Moreover, numerous studies have demonstrated that chromatin regulation is involved in the expression of stress-associated genes, including protein P21 (GRMZM2G039639_P01) and histone2A1 (GRMZM2G305046_P01), as well as the structural constituent of ribosome protein (GRMZM2G109677_P03).

Pb-stress alters the expression of proteins in lipid metabolism and redox pathways

MapMan analysis was used to evaluate whether significant DEPs with great alteration due

to Pb stress were clustered in specific metabolic pathways. As expected, there was an increase in abundance of many proteins involved in amino acid metabolism as well as lipid and hormone metabolism in response to Pb stress. Two proteins with increased expression were found to be involved in lipid synthesis. Lipid metabolism is affected by heavy metal-induced oxidative stress, in varying degrees depending on concentration and tissue types (Gao et al., 2010).

In addition, some DEPs were identified as regulators for redox pathways. In plants, cellular redox homeostasis can sense and transfer reducing equivalents to numerous target proteins, which is maintained by NAD(P) H-dependent thioredoxin and glutaredoxin systems and involved in various adverse environments (Meyer et al., 2012). In addition, several studies have revealed that glutathione (GSH) acts as an important protection system against metal stress in plants. In *Arabidopsis thaliana,* Vanhoudt et al. (2010) demonstrated that the redox balance of GSH plays a vital role in protecting against uranium and cadmium stress. In *Vicia faba*, GSH content was increased by mercury stress level and related to the elimination of H_2O_2 via the ascorbate GSH cycle (Wang et al., 2010). Kalinowska and Pawlik-Skowrońska (2010) also reported that maintenance of a higher level of GSH was responsible for a higher resistance to copper concomitant with phytochelatin production.

In summary, DEPs associated with Pb stress were identified in our iTRAQ studies and most of them were found to be involved in lipid metabolism and redox pathways. Further characterization of these Pb-regulated proteins may provide new insights into the molecular mechanism of action of lead pollution in plants.

Conflicts of interest

The authors declare no conflict of interest.

ACKNOWLEDGMENTS

Research supported by grants from the National Science Foundation of China (#31171567), the Research Project on Rice Functional Genes related to the Maize Large-scale Gene Discovery and Functional Genomics Resource, Technology, Information Platform Construction Program “863” of China (#SS2012AA100107 and #2012AA10A300), the Science and Information Technology Bureau of Guangzhou (#2013J2200083), the Guangdong Province and Ministry of Education Production-Study-Research Program of China (#2012B091100467), the Foundation of the President of the Guangdong Academy of Agricultural Sciences (201407), and the Guangdong Province Science and Technology Program (#2013B020301015).

REFERENCES

Atkinson NJ and Urwin PE (2012). The interaction of plant biotic and abiotic stresses: from genes to the field. *J. Exp. Bot.* 63: 3523-3543. http://dx.doi.org/10.1093/jxb/ers100

Beaudette PC, Chlup M, Yee J and Emery RJ (2007). Relationships of root conductivity and aquaporin gene expression in Pisum sativum: diurnal patterns and the response to HgCl2 and ABA. *J. Exp. Bot.* 58: 1291-1300. http://dx.doi.org/10.1093/jxb/erl289

Ding H, Gao J, Qin C, Ma H, et al. (2014). The dynamics of DNA methylation in maize roots under Pb stress. *Int. J. Mol. Sci.* 15: 23537-23554. http://dx.doi.org/10.3390/ijms151223537

Fan XD, Wang JQ, Yang N, Dong YY, et al. (2013). Gene expression profiling of soybean leaves and roots under salt, saline-alkali and drought stress by high-throughput Illumina sequencing. *Gene* 512: 392-402. http://dx.doi.org/10.1016/j.

gene.2012.09.100
Fetter K, Van Wilder V, Moshelion M and Chaumont F (2004). Interactions between plasma membrane aquaporins modulate their water channel activity. *Plant Cell* 16: 215-228. http://dx.doi.org/10.1105/tpc.017194
Gan CS, Chong PK, Pham TK and Wright PC (2007). Technical, experimental, and biological variations in isobaric tags for relative and absolute quantitation (iTRAQ). *J. Proteome Res.* 6: 821-827. http://dx.doi.org/10.1021/pr060474i
Gao J, Zhang Y, Lu C, Peng H, et al. (2015). The development dynamics of the maize root transcriptome responsive to heavy metal Pb pollution. *Biochem. Biophys. Res. Commun.* 458: 287-293. http://dx.doi.org/10.1016/j.bbrc.2015.01.101
Gao S, Ou-yang C, Tang L, Zhu JQ, et al. (2010). Growth and antioxidant responses in *Jatropha curcas* seedling exposed to mercury toxicity. *J. Hazard. Mater.* 182: 591-597. http://dx.doi.org/10.1016/j.jhazmat.2010.06.073
Guerra F, Duplessis S, Kohler A, Martin F, et al. (2009). Gene expression analysis of Populus deltoides roots subjected to copper stress. *Environ. Exp. Bot.* 67: 335-344. http://dx.doi.org/10.1016/j.envexpbot.2009.08.004
Guo L, Wang ZY, Lin H, Cui WE, et al. (2006). Expression and functional analysis of the rice plasma-membrane intrinsic protein gene family. *Cell Res.* 16: 277-286. http://dx.doi.org/10.1038/sj.cr.7310035
Kalinowska R and Pawlik-Skowrońska B (2010). Response of two terrestrial green microalgae (Chlorophyta, Trebouxiophyceae) isolated from Cu-rich and unpolluted soils to copper stress. *Environ. Pollut.* 158: 2778-2785. http://dx.doi.org/10.1016/j.envpol.2010.03.003
Meyer Y, Belin C, Delorme-Hinoux V, Reichheld JP, et al. (2012). Thioredoxin and glutaredoxin systems in plants: molecular mechanisms, crosstalks, and functional significance. *Antioxid. Redox Signal.* 17: 1124-1160. http://dx.doi.org/10.1089/ars.2011.4327
Miernyk JA and Hajduch M (2011). Seed proteomics. *J. Proteomics* 74: 389-400. http://dx.doi.org/10.1016/j.jprot.2010.12.004
Rea PA (1999). MRP subfamily ABC transporters from plants and yeast. *J. Exp. Bot.* 50: 895-913. http://dx.doi.org/10.1093/jxb/50.Special_Issue.895
Salt DE and Wagner GJ (1993). Cadmium transport across tonoplast of vesicles from oat roots. Evidence for a Cd2+/H+ antiport activity. *J. Biol. Chem.* 268: 12297-12302.
Salt DE and Rauser WE (1995). MgATP-dependent transport of phytochelatins across the tonoplast of oat roots. *Plant Physiol.* 107: 1293-1301.
Sheoran IS, Ross AR, Olson DJ and Sawhney VK (2009). Compatibility of plant protein extraction methods with mass spectrometry for proteome analysis. *Plant Sci.* 176: 99-104. http://dx.doi.org/10.1016/j.plantsci.2008.09.015
Tester M and Bacic A (2005). Abiotic stress tolerance in grasses. From model plants to crop plants. *Plant Physiol.* 137: 791-793. http://dx.doi.org/10.1104/pp.104.900138
Thapa G, Sadhukhan A, Panda SK and Sahoo L (2012). Molecular mechanistic model of plant heavy metal tolerance. *Biometals* 25: 489-505. http://dx.doi.org/10.1007/s10534-012-9541-y
Vanhoudt N, Vandenhove H, Horemans N, Wannijn J, et al. (2010). The combined effect of uranium and gamma radiation on biological responses and oxidative stress induced in *Arabidopsis thaliana*. *J. Environ. Radioact.* 101: 923-930. http://dx.doi.org/10.1016/j.jenvrad.2010.06.008
Valko M, Morris H and Cronin MT (2005). Metals, toxicity and oxidative stress. *Curr. Med. Chem.* 12: 1161-1208. http://dx.doi.org/10.2174/0929867053764635
Wang CR, Tian Y, Wang XR, Yu HX, et al. (2010). Hormesis effects and implicative application in assessment of lead-contaminated soils in roots of *Vicia faba* seedlings. *Chemosphere* 80: 965-971. http://dx.doi.org/10.1016/j.chemosphere.2010.05.049
Zelazny E, Borst JW, Muylaert M, Batoko H, et al. (2007). FRET imaging in living maize cells reveals that plasma membrane aquaporins interact to regulate their subcellular localization. *Proc. Natl. Acad. Sci. USA* 104: 12359-12364. http://dx.doi.org/10.1073/pnas.0701180104
Zhang Z, Jin F, Wang C, Luo J, et al. (2012). Difference between Pb and Cd accumulation in 19 elite maize inbred lines and application prospects. *J. Biomed. Biotechnol.* 2012: 271485 http://dx.doi.org/10.1155/2012/271485.

Supplementary material

Table S1. Elementary proteomics data of maize roots repsonsive to Lead (Pb) revealed by iTRAQ.

Table S2. Differentially expressed proteins involved in different metabolic pathways.

www.geneticsmr.com/year2016/vol15-1/pdf/gmr7254_supplementary.pdf